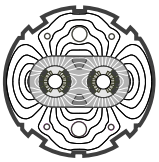

LHC Project Note 324

29 September 2003
Keith.Potter@cern.ch

Cascade simulations for the machine induced background study in the IR1 of the LHC

I. Azhgirey*, I. Baishev*, K.M. Potter and V. Talanov*

Keywords: losses, cascade, muon

Summary

In this note we present an analysis of the machine background formation in the interaction region IR1 of the LHC and results of a particle flux calculation at the entrance to the IP1 experimental region.

Introduction

The interactions of the beam particles with the nuclei of the residual gas in the LHC vacuum chamber are the main origin of the *machine induced background* — secondary particle flux that reaches the regions of the LHC collision points from the machine tunnel. The calculation of the machine induced background, made for the low luminosity LHC insertions IR2 and 8, showed the dependence of the resulting particle fluxes on the optics, the mechanical layout and the residual gas dynamics in the considered region of the machine structure. The various machine parameters were taken into account by using a specially developed methodical approach to the study of the machine background problem.

In this note we present an estimation of the machine induced background for the IP1 insertion region of the LHC. We analyze the formation of the background in the machine structure of this region and examine the relative contribution to the background from the different sections of the machine.

1 Simulation parameters and setup

The parameters of the simulation that define the considered machine layout are given in Table 1 below. We present the results obtained for the current version of the LHC optics

*Institute for High Energy Physics, Protvino, Russia.
Member of the Russian collaboration to the LHC Project.

in IR1 'at collision' and the nominal value of the circulating beam current. The transport threshold of 20 Mev kinetic energy, used in the calculations, enables most of the particles significant for the analysis of the radiation environment in the experimental zones to be taken into account.

LHC optics version	6.4
β^* in IP1 at collision	0.5 m
E_{kin} transport threshold	20 MeV
Circulating beam current	0.54 A

Table 1: Paramaters of the cascade simulations.

The choice of the LHC structure length considered in this study is based on the current understanding of the beam loss formation in the machine. As it was noted in [1], in the case of nominal operation of the LHC beam cleaning system only the part of the machine structure, located downstream from the cleaning insertion, between the cleaning and the collision point, needs to be considered. For the interaction point of IR1 this part consists of the two LHC sectors 78 and 81. Thus we present below the estimation of the machine background, which is induced in these sectors and reaches the entrance of the UX15 cavern of the IR1 collision point.

The cascade simulation was performed using one of the methodical approaches, developed by IHEP Radiation Physics Group for the solution of the radiation problems in the LHC project [2]. In this approach the proton losses are simulated along the considered LHC length, using the data on the residual gas composition and density in the different LHC elements. The products of these elastic and inelastic proton-nuclei interactions are transported through the machine structure and the resulting secondary cascades are simulated. The history of the cascade simulation is stopped at the entrance to the experimental region, where the coordinates of the particle track crossings with some imaginary 'scoring' plane are recorded for future analysis.

The s position of this fictitious plane, which is perpendicular to the beam axis, was chosen to include the whole length of the IR1 inner triplet, the closest to the IP and known to be the most important element of the machine structure. According to the LHC optics version 6.4, the front surface of the inner triplet Q1 quadrupole is located at 22.965 m from the IP1. The positioning of the scoring plane had also to take into account the IP1 inner shielding layout, an illustration of which is given in Figure 2. From this drawing it can be seen that the most effective position for the scoring plane is the distance of 23 m from the IP1. The plane at this position includes the Q1 magnet material and coincides with the front surface of the concrete shielding, thus simplifying the geometry setup of the simulation. As shown on Figure 3, this chosen plane cuts the fixed tube of the inner shielding, so that only that element together with the concrete block had to be introduced in the standard model of the simulations, which consisted of the machine structure elements and LHC tunnel, surrounding them [2]. In this standard model all the necessary details of the beam line structure, such as the beam screen inside the magnets and the layout of the interconnections were taken into account. Cascade simulations were performed for beam one over the length of the two LHC sectors, including the left part of the IR1 straight section itself. Since IR1 is symmetrical

with respect to the surrounding low luminosity collision regions and cleaning insertions, the results of the simulations are also valid for the opposite side of the collision point and beam two.

2 Residual gas density profile in IR1

The values for the residual gas composition and density are one of the important parameters of the machine background simulations. For the present study these values were taken from the most recent, available estimations of these quantities for the different regions of the LHC structure [3]. An extract from this reference is given in Table 2 for several specific elements of IR1, together with the element lengths that have to be taken into account to obtain the relative contribution from a particular element. As can be seen from Table 2, the lowest gas density value of 10^{12} mol/m^3 corresponds to the longest warm 'conus' drift between two separation dipoles D1 and D2. This means that with the current estimations this section of IR1 contributes to the final background only because of its significant length of 57 m. But in the case of an increased gas density in this region for whatever reason, this part can become the primary source, since it consists of 1/5 of the whole straight section length.

Element	**L, [m]**	$\mathbf{n}_{H_2}$**, [mol/m^3]**	**Element**	**L, [m]**	$\mathbf{n}_{H_2}$**, [mol/m^3]**
Q1	7.70	6×10^{12}	'Conus'	≈ 57	10^{12}
Intercon.	1.40	1.5×10^{14}	D2	11.67	1.5×10^{14}
Q2	12.58	3×10^{12}	Q4	8.65	2×1013
Intercon.	1.90	1.5×10^{14}	VC (RT)	19.38	5×10^{12}
Q3	8.40	6×10^{12}	DFBA	8.58	5×10^{12}
DFBX	3.23	1.5×10^{14}	DS & Arc		4×10^{12}
D1 (RT)	≈ 25	5×10^{12}			

Table 2: Hydrogen equivalent gas density in the IR1 elements.

For the IR1 & 5 of the LHC the values in Table 2 differ at least for a couple of locations from the estimations, used for the study of the machine background in the low luminosity insertion regions of the LHC [4]. Since the level of the residual gas density directly gives the rate of the primary proton-nucleus interactions which are the source of the background, this difference is one of the causes that determines the specific behavior and absolute rate of the machine induced background in IR1.

One of these locations is the first separation dipole D1 of the straight section. This dipole is a cold MBX magnet for the low luminosity insertions, so in the IR2 & 8 this dipole is featured by the same hydrogen equivalent gas density value of 1.5×10^{14} mol/m^3, as for the second separation dipole D2 and DFBA/X boxes. For the high luminosity insertion regions the type of this dipole is a warm MBXW magnet, which has a significantly lower value for the gas density of 5×10^{12} mol/m^3. Another important difference is in the DFBA box downstream of the Q7 quadrupole in the matching section. The value for this box in [3] was calculated for the LHC optics version 6.3, were the beam pipe inside this element was at cryogenic temperature. We present the results of the simulations for the current LHC optics

version 6.4, where the vacuum chamber in this region is moved out from the cryostat, so the nominal value for a warm drift in the matching section of 5×10^{12} mol/m^3 was used for this element.

These differences result in a visible change of the residual gas density distribution in the IR1, with respect to the IR2 & 8. The assumed decreased values for the matching and separation section elements determine the lower contribution from the straight section in the IR1 to the total particle flux. Together with the assumed very low value of 4×10^{12} mol/m^3 for the gas density in the dispersion suppressor and arc elements this fact allows one to presume that the absolute value of the machine induced background in IR1 will be even lower than for IR2 & 8.

3 Secondary particle flux from the LHC tunnel at the UX15 entrance

The result of the cascade simulations for the machine background study in the IR1 was recorded as a source of the secondary particles at the entrance of the UX15 cavern. The absolute values for hadron and muon fluxes, obtained by the integration over this source, are given in Table 3 below. The relative ratio between hadrons and muons appears to be of about an order of magnitude which is the same as for the low luminosity insertions, and the absolute flux values are comparable to those for IR2 & 8, assuming the nominal value of the gas density for the TDI region [5].

Hadrons			**Muons**		
Total	LSS	Ratio	Total	LSS	Ratio
1.77×10^6	1.57×10^6	89 %	1.04×10^5	6.77×10^4	65 %

Table 3: Particle fluxes — total and from straight section SS only, and their ratio.

Meanwhile cryogenic and warm parts of the considered LHC length contribute to the total particle flux from the IR1 in a proportion, somewhat different from the previously studied low luminosity insertion regions. Together with the total values for the whole accounted length, Table 3 gives the fraction of hadrons and muons, produced in the secondary cascades from the interactions in the straight section only. The difference between these two values is by definition the contribution from the dispersion suppressor and the cold arcs. This fraction is already visible for hadrons, where it is about 10 % of the total flux. For muons the contribution from the straight section alone with regard to the fluxes in the IR2 & 8 is decreased because of the absence in IR1 of the two cold elements with the highest estimated values for the gas density, as was pointed in the previous section.

At the same time, comparing to the low luminosity insertions, the role of the cold DS and arc sections is increased significantly for muons. Previously for IR2 & 8 with the new data for the residual gas density [3] the contribution to the background from the cryogenic parts of the LHC was estimated as negligible. So the straight section of the IR2 & 8 alone was considered as the length of the machine structure, which allowed a rather complete

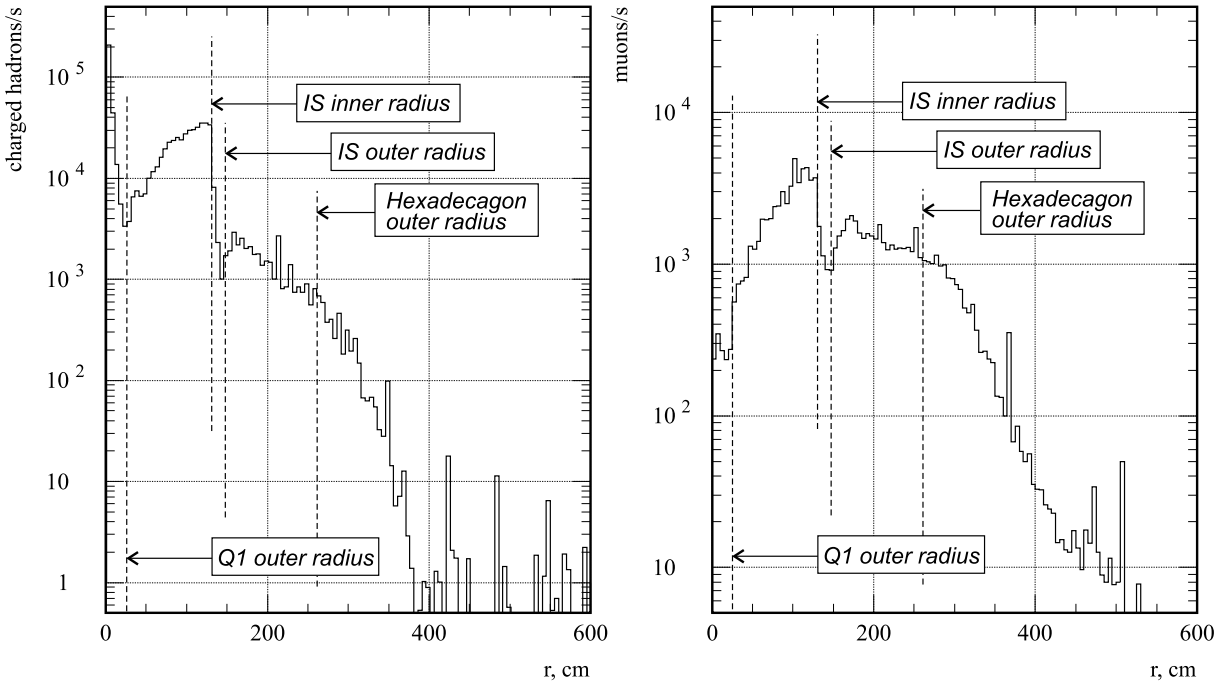

Figure 1: Radial distributions of charged hadron (left) and muon (right) flux at the UX15 entrance. Vertical lines on the plots show the limits of the material of the different elements — Q1 magnet, fixed tube of the inner shielding and hexadecagon of the outer one.

study of the machine induced background problem in these insertion regions [5]. It appears not to be the case for the high luminosity IR1 where even for the very low gas density of 4×10^{12} mol/m^3 the proton losses in the cold magnets of the dispersion suppressor and arc determine about 30 % of the total muon flux at the entrance to the UX15 cavern. This fact is the reflection of a more demanding optical structure of IR1 [6], which collects more particles from the upstream elastic proton-nucleus interactions, than for IR8 and especially IR2 with $\beta^* = 10$ m in the inner triplet [7].

It has to be noted that the values for the particle fluxes are given in Table 3 at the position of the source scoring plane. According to Section 1 of the present note, the position of the scoring plane was defined so that it crossed the shielding of IP1. This means that the secondary particles, recorded at that location, will be additionally attenuated by the material of the downstream shielding elements before they reach the experimental area of IR1 itself. This fact is illustrated by Figure 1, where the radial distribution of the charged hadron flux and muon flux at the scoring plane are given. As shown on this figure, the fraction of the secondary particles, which is within the radius of the inner shielding fixed tube, will encounter in addition the material of the TAS collimator, the cradle and monobloc. The particles beyond this radius, up to a distance of 2.6 m from the beam line, will have to pass through the ≈ 2 m thick iron plates that make up the hexadecagon of the TX1S outer shielding. Only the fraction of the particle flux which comes above the outer shielding radius will reach the experimental area of IR1 directly.

4 Particle flux formation in the straight section of IR1

Despite the relatively increased contribution to the total particle flux from the cold dispersion suppressor and arc sections, the major portion of the secondary particles is still produced in the straight section of IR1. An analysis of the formation of this background component is illustrated by the Figures 4 and 5. These figures present the distribution of hadrons and muons, produced in the elastic and inelastic interactions in the SS of IR1, as a function $N(s)$ of the interaction distance to the IP1. To associate these distributions with the values for the residual gas densities in the straight section elements from Table 2, at the top of each plot, the drawing of the LSS optical structure is given. The bullets on each curve correspond to the center of the particular element of the structure.

The two curves, given on each figure, represent the same integrated values for the particle flux. The solid curve gives the distribution of the particle flux along the straight section as a function of the primary proton-nucleus collision distance to the center of the IR1. These curves show the locations in the SS where most of the primary beam-gas interactions occur. The dashed curve gives the distribution of the particle parent vertexes in the straight section and show the direct origin of the background — the locations in the SS where the last hadron-nucleus interaction occurred which gave a particle track that fell into the recorded source, for a muon or, a parent pion.

The primary beam-gas interaction does not always give the particles which will be seen at the entrance of the UX15 but rather determines the secondary flux through the subsequent cascades in the straight section. For both hadrons and muons these two curves are different for the regions located close to the IP1 and those farther away. Both hadron and muon distributions have a central peak in the D2 region, which reflects the high value of the residual gas pressure there. Downstream of D2, in the D1 and inner triplet section, the contribution to hadrons from the different elements increases with the decrease of the distance to the IP1. The observed oscillations in the region of Q1–DFBX reflect the assumed profile for the gas pressure in these elements, where for the cold interconnections in the inner triplet the values are about 20 times higher than for the magnets they connect. As can be seen from the parent hadron vertex distribution, the material of the inner triplet magnets effectively shields the beam-gas interactions inside the vacuum chamber, and only the particles produced in the material of the Q1 quadrupole have a chance to reach the UX15 cavern. Upstream of D2, the contribution from the matching section elements is low, for the assumed decreased value for the DFBA box, and the direct contribution from the parent vertexes there is lower by an order of magnitude.

For the muons downstream of D2, the closer to the IP1, the less is the relative role of the particular structure element, since the process of muon production requires an open space for the parent pion to decay to a muon. So the beam-gas interactions directly inside the inner triplet give less contribution to the muon final flux than for the hadrons. Upstream of D2, in the matching section, the source of muons consists of the interactions on the vacuum chamber with a subsequent decay length between the quadrupoles. The most important region for the muon production appears to be the long warm drift between the separation dipoles D1 and D2. Due to the lowest gas density value for this element, this element contributes directly to the observed background only because it is a relatively long part of the structure. In the same time, this part of the SS provides a long open space, not shielded

by the material of the magnets, for the scattered particles to escape from the beam aperture and interact then with the vacuum chamber or the outer part of the D1 dipole. So for the muons this appears to be the region where most of these particles that reach the entrance to the experimental cavern are produced.

Conclusion

In this note we analyze the formation of the machine induced background in IR1 of the LHC. We have estimated the values for the particle fluxes at the beam entrance to the UX15 experimental cavern, induced by the proton losses due to the beam-gas interactions in the LHC sectors 78 and 81, including the length of the left straight section of the IR1. The results show a total particle flux of 1.75×10^6 hadrons and 1.05×10^5 muons, for the current estimations of the residual gas pressure in the machine. With these estimations, the machine background in IR1 is determined by the gas pressure level in the cryogenic elements, of which separation dipole D2 and inner triplet box DFBX are the most important ones. Nevertheless, even with the assumed very low density for the dispersion suppressor and cold arc elements, the distant regions of the machine contribute visibly to hadrons and very significantly, for muons, up to one-third of the total particle flux. Thus considering this part in the machine background estimations appears to be still an important issue for the high luminosity insertions.

References

[1] I. Baichev, J.B. Jeanneret and K.M. Potter. *Proton losses upstream of IP8 in LHC.* CERN LHC Project Report 500, Geneva, 2001.

[2] I. Azhgirey, I. Baishev, K.M. Potter *et al. Methodical Study of the Machine Induced Background in the IR8 of LHC.* CERN LHC Project Note 258, Geneva, 2001.

[3] I.R. Collins and O.B. Malyshev. *Dynamic Gas Density in the LHC Interaction Regions 1&5 and 2&8 for Optics Version 6.3.* CERN LHC Project Note 274, Geneva, 2001.

[4] I. Azhgirey, I. Baishev, K.M. Potter *et al. Machine Induced Background in the Low Luminosity Insertions of the LHC.* CERN LHC Project Report 567, Geneva, 2002. Pres. at: 8th European Particle Accelerator Conference: a Europhysics Conference, La Vilette, Paris, France, 3–7 June 2002.

[5] I. Azhgirey, I. Baishev, K.M. Potter *et al. Calculation of the Machine Induced Background in the IR2 of LHC Using New Residual Gas Density Distributions.* CERN LHC Project Note 273, Geneva, 2001.

[6] O. Bruening *et al. A Beam Separation and Collision Scheme for IP1 and IP5 at the LHC for Optics Version 6.1.* CERN LHC Project Report 315, Geneva, 1999.

[7] O. Bruening *et al. A Beam Separation and Collision Scheme for IP2 and IP8 at the LHC for Optics Version 6.1.* CERN LHC Project Report 367, Geneva, 2000.

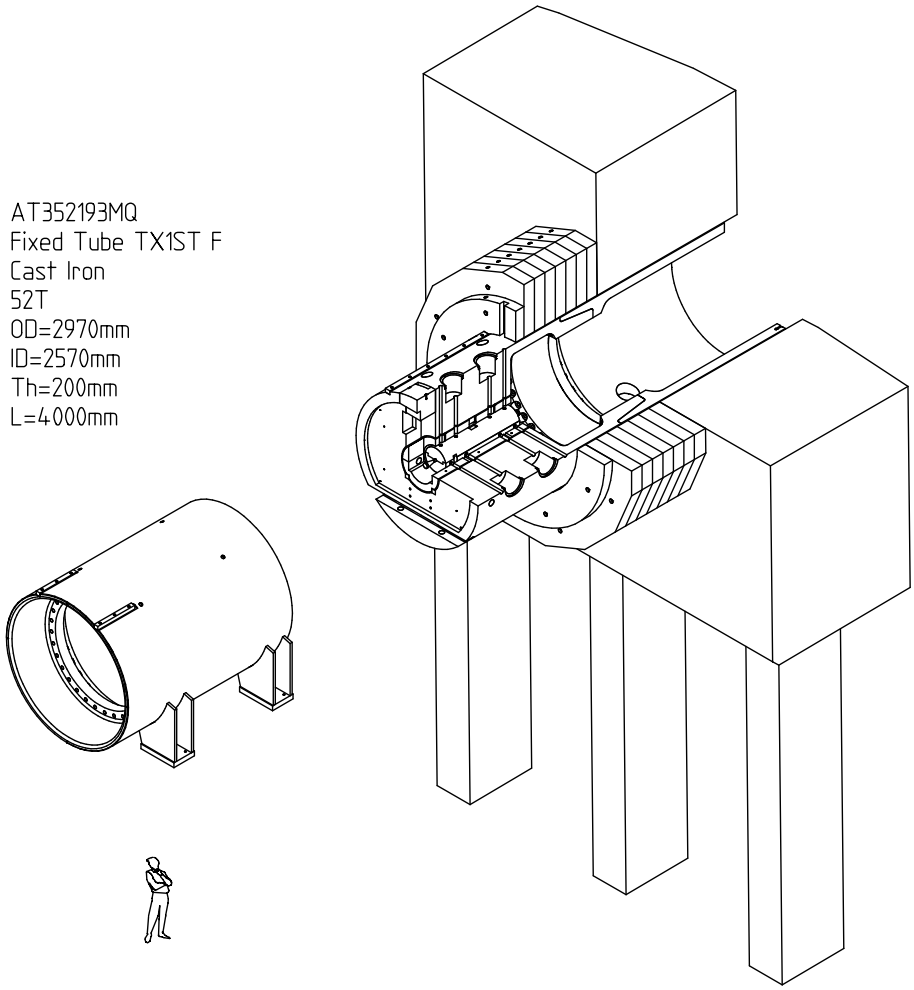

Figure 2: An extract from the drawing `LHCTX1S_0002` that shows the section of the UX15 inner shielding together with its fixed tube part.

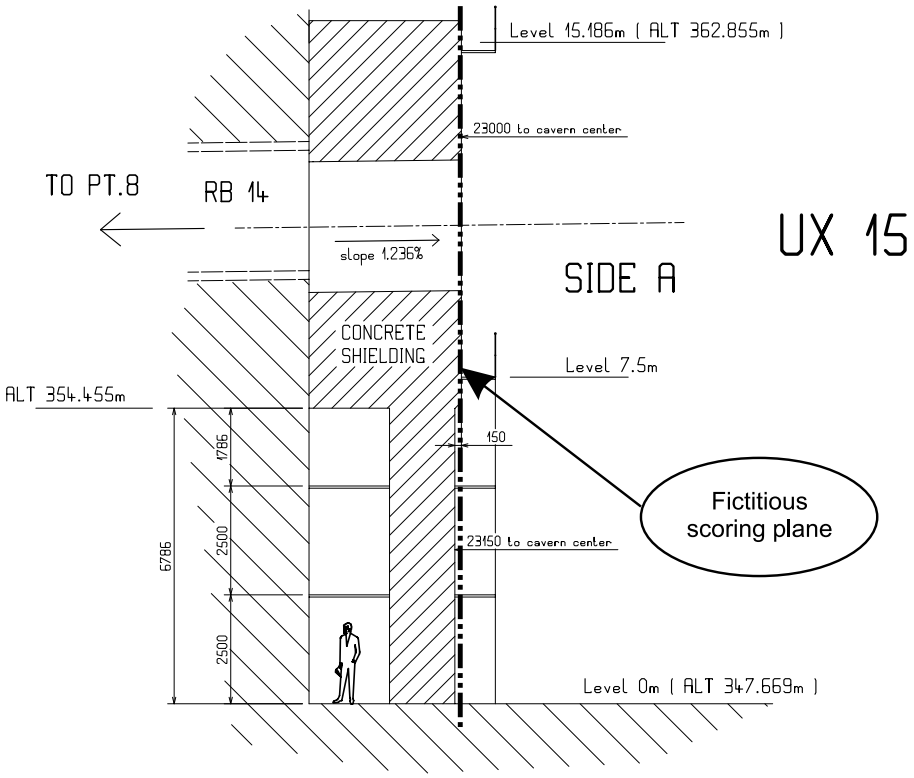

Figure 3: An extract from the drawing `LHCJUX150003` that shows the LHC tunnel opening into the UX15 cavern and the position of the plane, where the particle source was recorded.

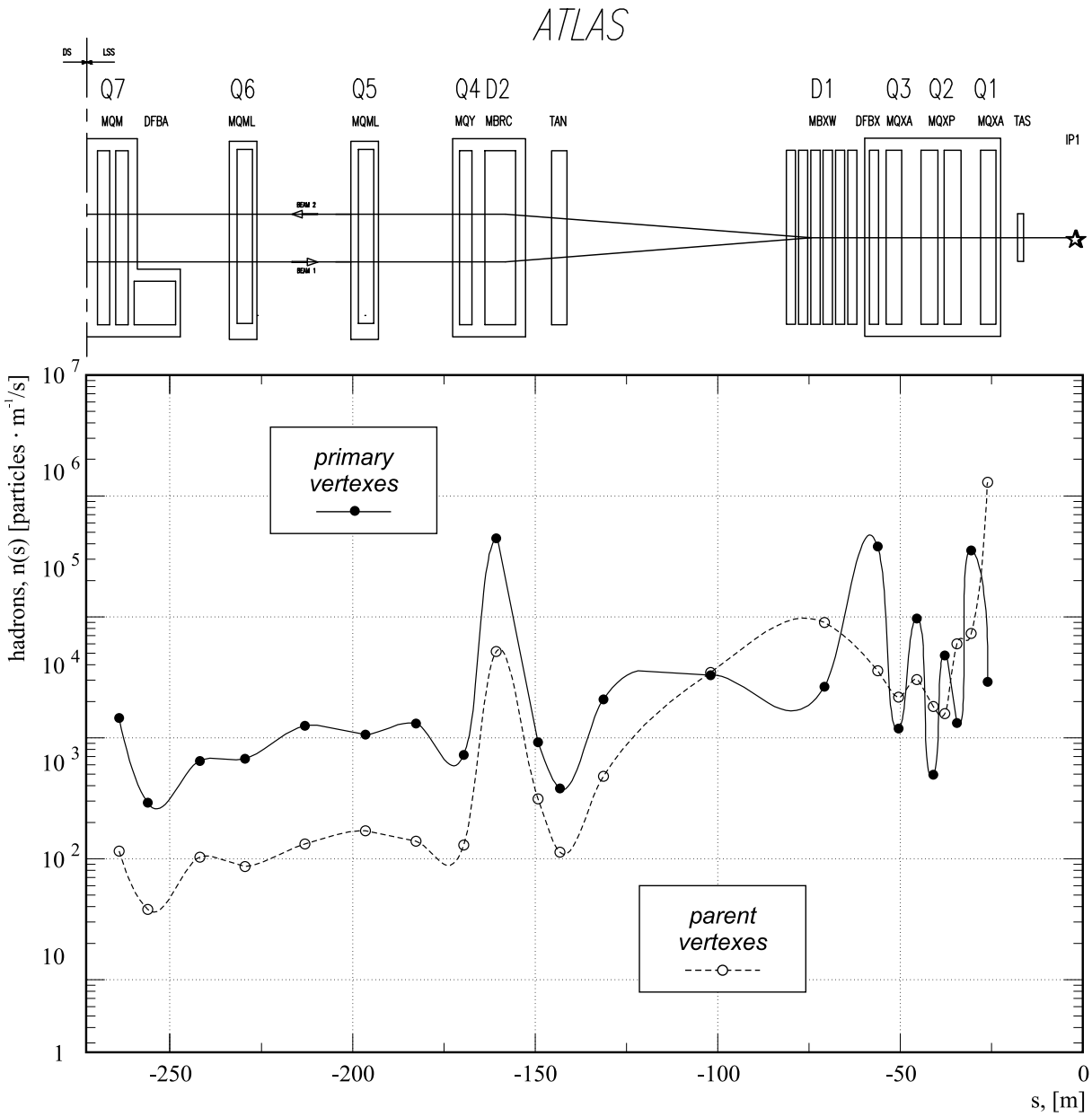

Figure 4: Number of hadrons as a function of primary (solid) and last (dashed) proton–nucleus interaction distance to IP1.

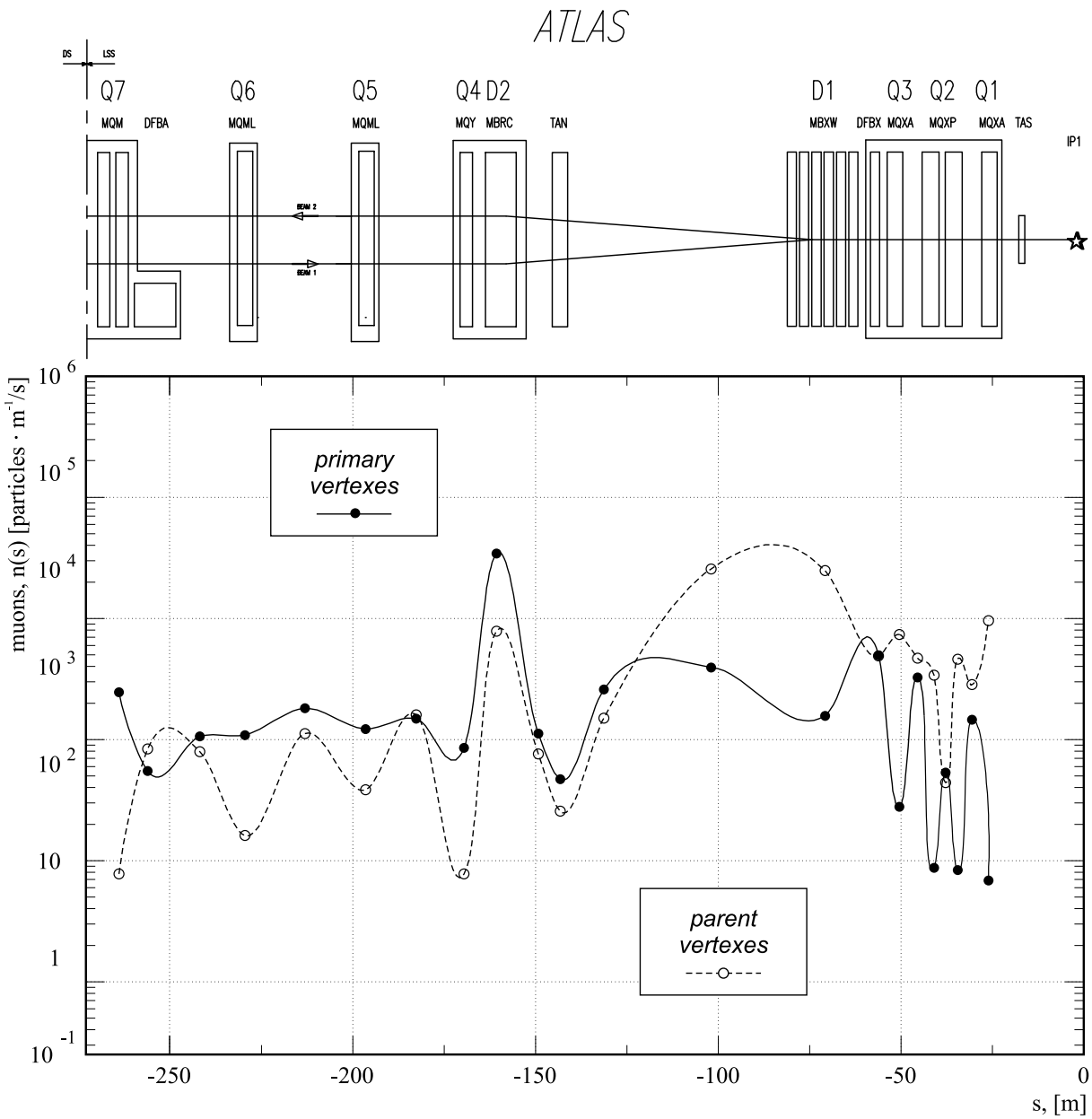

Figure 5: Number of muons as a function of primary (solid) and last (dashed) proton–nucleus interaction distance to IP1.